

Article

Synthesis, Crystal Structure, and Optical Properties of Mononuclear Eu(III) and Tb(III) Complexes Containing a Chalcone Ligand

Valentin L. Virgil¹, Anamaria Hanganu^{1,2}  and Augustin M. Mădălan^{1,*}

¹ Faculty of Chemistry, University of Bucharest, 4-12 Regina Elisabeta Blvd., 030018 Bucharest, Romania; valentin.virgil@s.unibuc.ro (V.L.V.); anamaria_hanganu@yahoo.com (A.H.)

² “Costin D. Nenițescu” Institute of Organic and Supramolecular Chemistry of the Romanian Academy, 202B Splaiul Independentei, 060023 Bucharest, Romania

* Correspondence: augustin.madalan@chimie.unibuc.ro

Abstract: Chalcones are α,β -unsaturated ketones with great structural diversity and various applications. A chalcone produced by condensation of 2-acetylpyridine with 2-naphthaldehyde (L) was employed for synthesis of two mononuclear complexes: $[\text{Eu}(\text{L})(\text{hfac})_3(\text{H}_2\text{O})] \cdot 0.5\text{CHCl}_3$ and $[\text{Tb}(\text{L})(\text{hfac})_3]$, where hfac is the hexafluoroacetylacetonate anion. The chalcone and complexes were structurally characterized by single-crystal X-ray diffraction. The chalcone acts as a chelating bidentate ligand. Luminescent properties of the ligand L and the complexes were investigated in the solid state. For these heteroleptic mononuclear complexes, the emission of the Eu(III) and Tb(III) ions was influenced by the excitation wavelength.

Keywords: chalcone; lanthanide complexes; heteroleptic complexes; luminescence



Citation: Virgil, V.L.; Hanganu, A.; Mădălan, A.M. Synthesis, Crystal Structure, and Optical Properties of Mononuclear Eu(III) and Tb(III) Complexes Containing a Chalcone Ligand. *Crystals* **2023**, *13*, 1406. <https://doi.org/10.3390/cryst13091406>

Academic Editor: Vadim Yu. Kukushkin

Received: 21 August 2023

Revised: 16 September 2023

Accepted: 20 September 2023

Published: 21 September 2023



Copyright: © 2023 by the authors. Licensee MDPI, Basel, Switzerland. This article is an open access article distributed under the terms and conditions of the Creative Commons Attribution (CC BY) license (<https://creativecommons.org/licenses/by/4.0/>).

1. Introduction

Chalcones are α,β -unsaturated ketones showing great structural diversity. Many chalcones are naturally occurring compounds with a widespread distribution in plants. Synthetic chalcones attract considerable interest due to the potential biomedical applications related to their biological activities: anticancer, anti-inflammatory, antioxidant, antimicrobial, antidiabetic, and others [1]. Chalcones are relatively easily accessible via Claisen–Schmidt condensation of an aromatic aldehyde with an aliphatic aldehyde or ketone in basic or acid conditions. Chalcones are valuable precursors for synthesis of various organic compounds undergoing different types of reactions: diastereo- and enantioselective cross-cascade reactions [2], cyclization [3], hydroacylation [4], and condensation [5]. The α,β -unsaturated ketone fragment, as a polar π system connecting two different aromatic moieties, can be used to induce nonlinear optical properties. Depending on the electron donor or electron acceptor capabilities of the two aromatic moieties connected by the α,β -unsaturated ketone fragment, three types of systems can be obtained: donor- π -donor (D- π -D), acceptor- π -acceptor (A- π -A), and donor- π -acceptor (D- π -A). For the chalcones containing anthracene (the electron-rich group) and pyridine or pyrazine (the electron-deficient groups), the nonlinear optical properties were influenced by the coordination of the pyridine/pyrazine N atoms to transitional metal ions [6]. The two-photon absorption process (as a third-order nonlinear optical phenomenon) for bis-chalcones derived from 2,6-diacetylpyridine can be enhanced by the interaction with Mg(II), Ca(II), or Zn(II) metal ions [7]. Also, bis-chalcones derived from 2,6-diacetylpyridine have been used as fluorescent sensors for Fe(III) ions [8].

The coordination abilities of chalcones can be enhanced by the presence of heteroatoms (O or N) that are favorably positioned in order to generate chelatic rings by coordination with the metal ion together with the ketone O atom. The chalcone derived

from 2'-hydroxyacetophenone and 4-(dimethylamino)benzaldehyde was used for synthesis of a luminescent homoleptic Be(II) complex [9]. In this complex, the chalcone coordinates as chelating bidentate ligand, and the emissive properties are influenced by the aggregation modes of the mononuclear complexes. Other chalcones derived from 2'-hydroxyacetophenone were employed for synthesis of heteroleptic Cu(II) [10–13], Zn(II) [13], Ni(II) [14], or Ru(II) complexes [15–18]. These chalcones also act as chelating bidentate monoanionic ligands (by deprotonation of the phenol group). The flat nature of chalcone ligands with extended π systems makes these complexes suitable for DNA binding [16,18]. Chalcones derived from 2-acetylpyridine and various aromatic aldehydes can also coordinate chelating bidentate, but examples of such complexes structurally characterized by single-crystal X-ray diffraction are still scarce. A search in the Cambridge Structural Database (CSD) revealed only two examples: a Pd(II) complex [19] and an Eu(III) complex [20]. The metal ions are coordinated chelating bidentate by the pyridine N atom and the ketone O atom of the chalcone ligands. In a Pt(II) compound, the interaction of the metal ion with the chalcone derived from 2-acetylpyridine and 9-anthracenecarboxaldehyde involves the pyridine N atom and the carbon–carbon double bond [21].

In this paper, we reported on the synthesis and structural characterization by single-crystal X-ray diffraction of the chalcone obtained by condensation of 2-acetylpyridine with 2-naphthaldehyde (L) and of two heteroleptic lanthanide(III) complexes, containing this chalcone and hexafluoroacetylacetonate anion (hfac) as chelating ligands, [Eu(L)(hfac)₃(H₂O)]·0.5CHCl₃, and [Tb(L)(hfac)₃]. The photoluminescent properties of the ligand L and complexes were investigated on solid samples.

2. Materials and Methods

2.1. Synthesis

The chemicals and solvents used were of reagent grade and were purchased from commercial sources (Sigma-Aldrich, Merck, Honeywell, Charlotte, NC, USA). The lanthanide tris-hexafluoroacetylacetonato compounds were obtained according to the reported procedures [22].

2.1.1. Synthesis of the Ligand L

A mixture containing 3 mmol of 2-acetylpyridine, 3 mmol of 2-naphthaldehyde, and 2 mmol of KOH in 25 mL ethanol was stirred for two hours at room temperature. The yellow precipitate was filtered, washed with ethanol, and dried out. Yield: 75%. ¹H-NMR (500 MHz, DMSO-*d*₆, δ ppm, J Hz): 8.82 (d, 1H, H_{Py}, 4.6 Hz), 8.39 (d, 1H, -CH=, 16.1 Hz), 8.34 (s, 1H, H_{naphthyl}), 8.12 (d, 1H, H_{naphthyl}, 7.8 Hz), 8.06 (td, 1H, H_{Py}, 1.6 Hz, 7.6 Hz), 8.02–7.94 (m, 5H, -CH=, H_{naphthyl}, and H_{Py}), 7.70 (m, 1H, H_{Py}), 7.59–7.55 (m, 2H, H_{naphthyl}) ppm (the ¹H-NMR spectrum is presented in Figure S1). Selected IR data (KBr pellet, cm⁻¹): 1670 s, 1605 vs, 1593 s, 1577 s, 1434 m, 1360 m, 1315 s, 1269 m, 1243 m, 1209 m, 1175 w, 1042 m, 1037 s, 993 w, 980 s, 955 w, 867 w, 855 m, 814 m, 795 s, 761 w, 739 m, 688 m, 673 m, 618 m, 470 m, 434 w, 424 w, 415 m, 405 m.

2.1.2. Synthesis of the Complex [Eu(L)(hfac)₃(H₂O)]·0.5CHCl₃ (C1)

An amount of 0.1 mmol of the ligand L and 0.1 mmol of [Eu(hfac)₃(H₂O)₂] were dissolved in 40 mL mixture of heptane–chloroform (1:1) and stirred (350 rpm) for one hour at room temperature. The resulting solution was left for slow evaporation at room temperature. The yellow crystals of the complex [Eu(L)(hfac)₃(H₂O)]·0.5CHCl₃ were formed after three to five days. These were collected by filtration prior to the total evaporation of the solvents in order to avoid contamination with side products. At the moment of filtration, no precipitate was observed in the beaker. Yield: 60%. Selected IR data (KBr pellet, cm⁻¹): 3507 w, 1652 s, 1580 m, 1561 s, 1533 s, 1504 s, 1440 w, 1367 w, 1257 vs, 1203 vs, 1144 vs, 1066 w, 1008 w, 985 w, 849 m, 796 w, 740 w, 680 m, 661 w, 585 m, 527 w, 474 w.

2.1.3. Synthesis of the Complex [Tb(L)(hfac)₃] (C2)

A solution containing 0.1 mmol of the ligand L and 0.1 mmol of [Tb(hfac)₃(H₂O)₂] in 40 mL mixture of heptane–chloroform (1:1) was stirred (350 rpm) for one hour at room temperature. By slow evaporation at room temperature, the yellow crystals of the complex [Tb(L)(hfac)₃] appeared after several days and were collected by filtration prior to the total evaporation of the solvents. Yield: 65%. Selected IR data (KBr pellet, cm^{−1}): 1651 s, 1579 s, 1559 m, 1533 s, 1499 m, 1369 w, 1260 vs, 1211 vs, 1145 vs, 1069 m, 1011 w, 849 m, 798 w, 766 w, 742 w, 680 m, 660 w, 587 m, 471 w.

The purity of the crystalline samples was verified by powder X-ray diffraction (Figures S4–S6). For the chalcone, there was a good agreement between the experimental XRPD pattern and the simulated one from the single-crystal data (Figure S4). For the complex [Eu(L)(hfac)₃(H₂O)]·0.5CHCl₃ (C1), a loss of crystallinity over time was observed (Figure S5). The crystal structure presented solvent-accessible voids containing disordered chloroform molecules. The loss of solvent determines the crystal break. For each sample of the complexes C1 and C2, we collected only crystals, and we measured the unit cell for five to seven crystals to verify the purity.

2.2. Physical Measurements

2.2.1. X-ray Structure Determination

X-ray diffraction measurements were performed on a Rigaku XtaLAB Synergy-S diffractometer operating with Mo-Kα (λ = 0.71073 Å) micro-focus sealed X-ray tube. The structures were solved by direct methods and refined by full-matrix least squares techniques based on *F*². The non-H atoms were refined with anisotropic displacement parameters. Calculations were performed using SHELX-2018 crystallographic software package. A summary of the crystallographic data and the structure refinement are provided in Table 1. CCDC reference numbers: 2287899–2287901. CCDC contains the supplementary crystallographic data for the three compounds. These data can be obtained free of charge via <http://www.ccdc.cam.ac.uk/conts/retrieving.html>; from the Cambridge Crystallographic Data Centre, 12 Union Road, Cambridge CB2 1EZ, UK, fax: (+44)-1223-336-033; or by e-mail: deposit@ccdc.cam.ac.uk.

Table 1. Crystallographic data, details of data collection, and structure refinement parameters for the ligand L and complexes C1 and C2.

| Compound | L | C1 | C2 |
|---|------------------------------------|---|--|
| Chemical formula | C ₁₈ H ₁₃ NO | C _{33.5} H _{18.5} Cl _{1.5} EuF ₁₈ NO ₈ | C ₃₃ H ₁₆ F ₁₈ NO ₇ Tb |
| M (g mol ^{−1}) | 259.29 | 1110.13 | 1039.39 |
| Temperature, (K) | 293(2) | 293(2) | 293(2) |
| Wavelength, (Å) | 0.71073 | 0.71073 | 0.71073 |
| Crystal system | <i>Monoclinic</i> | <i>Triclinic</i> | <i>Triclinic</i> |
| Space group | <i>P2₁/n</i> | <i>P-1</i> | <i>P-1</i> |
| <i>a</i> (Å) | 14.4100(8) | 12.7861(5) | 14.3064(3) |
| <i>b</i> (Å) | 4.6748(3) | 13.4613(3) | 15.4744(3) |
| <i>c</i> (Å) | 19.6977(12) | 14.0329(5) | 18.5376(3) |
| <i>α</i> (°) | 90 | 112.470(3) | 101.683(2) |
| <i>β</i> (°) | 93.195(5) | 91.204(3) | 98.786(2) |
| <i>γ</i> (°) | 90 | 109.485(3) | 105.663(2) |
| <i>V</i> (Å ³) | 1324.85(14) | 2073.31(13) | 3774.87(13) |
| <i>Z</i> | 4 | 2 | 4 |
| <i>D_c</i> (g cm ^{−3}) | 1.300 | 1.778 | 1.829 |
| <i>μ</i> (mm ^{−1}) | 0.081 | 1.738 | 2.009 |
| <i>F</i> (000) | 544 | 1082 | 2016 |
| Goodness of fit on <i>F</i> ² | 1.031 | 1.059 | 1.062 |
| Final <i>R</i> ₁ , <i>wR</i> ₂ [<i>I</i> > 2σ(<i>I</i>)] | 0.0383, 0.1032 | 0.0415, 0.1140 | 0.0398, 0.1080 |
| <i>R</i> ₁ , <i>wR</i> ₂ (all data) | 0.0502, 0.1141 | 0.0456, 0.1179 | 0.0485, 0.1140 |

The X-ray powder diffraction (XRPD) measurements were carried out on a Proto AXRD Benchtop using the Cu-K α radiation with a wavelength of 1.54059 Å in the 2 θ range of 5–35°.

2.2.2. Spectroscopy

Absorption spectra on solid samples were measured using diffuse reflectance technique with a JASCO V-670 spectrophotometer. The fluorescence spectra were collected on powder using a JASCO FP-6500 spectrofluorometer.

The ^1H NMR spectra were measured in DMSO- d_6 using a Bruker Advance spectrometer operating at 500 MHz. The chemical shifts δ are reported as ppm values and the residual solvent peaks were used as an internal reference.

The IR spectra were recorded on KBr pellets using a Bruker Tensor 37 spectrophotometer in the 4000–400 cm^{-1} region. The following abbreviations were used: w = weak, m = medium, s = strong, v = very.

3. Results

The reaction of 2-acetylpyridine with 2-naphthaldehyde in ethanol in a basic condition generates the chalcone ligand L. Suitable single crystals for X-ray diffraction of the ligand L were obtained by slow evaporation of the solution containing this chalcone dissolved in a mixture of heptane and chloroform (1:1). Following the reaction of the ligand L with $[\text{Ln}(\text{hfac})_3(\text{H}_2\text{O})_2]$, Ln(III) = Eu(III), or Tb(III), two mononuclear complexes were obtained, $[\text{Eu}(\text{L})(\text{hfac})_3(\text{H}_2\text{O})] \cdot 0.5\text{CHCl}_3$ and $[\text{Tb}(\text{L})(\text{hfac})_3]$, respectively. The hexafluoroacetylacetonato anion (hfac) acts as an electron withdrawing ligand, and it was used to increase the chance of the chalcone ligand to coordinate to the lanthanide ions.

3.1. Crystal Structures' Description

The ligand L crystallizes in the monoclinic $P2_1/n$ space group with one molecule in the asymmetric unit. The molecular structure of the chalcone is presented in Figure 1. The two aromatic systems (the pyridyl and naphthyl fragments) within the molecule are not coplanar. The dihedral angle between the mean planes of the pyridyl and naphthyl fragments is 26.2°. The bond lengths for the C6–O1 and C7–C8 bonds are 1.2186(16) and 1.325(2) Å, confirming their double-bond nature.

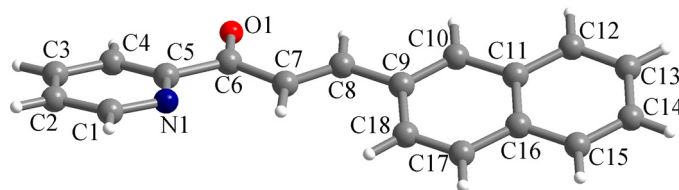


Figure 1. Perspective view of the molecular structure of L along with atom labelling scheme.

The molecules are organized in piles running along the crystallographic b axis (Figure 2). Within a pile, the naphthyl fragment of one molecule establishes π - π interactions with the naphthyl fragments of neighboring molecules with separations of 3.47–3.55 Å (the inset of Figure 2). The pyridyl moieties are involved in π - π interactions with the pyridyl fragments of neighboring molecules (3.54–3.64 Å) and, also, with the C–C double bond of one neighboring molecule (3.23 Å).

The complex $[\text{Eu}(\text{L})(\text{hfac})_3(\text{H}_2\text{O})] \cdot 0.5\text{CHCl}_3$ (C1) crystallizes in the triclinic $P-1$ space group with one molecule of the mononuclear Eu(III) complex and half of the chloroform molecule in the asymmetric unit. The chloroform molecule is disordered on two crystallographic positions (related by symmetry) with site occupancy factors of 0.5 each. In complex C1, the Eu(III) ion presents the coordination number nine with four chelating bidentate ligands (three hfac anions and one chalcone L) and one water molecule (Figure 3a). The chalcone L coordinates through the pyridine N atom and the ketone O atom. The corresponding bond lengths are: Eu1–N1 = 2.612(4) and Eu1–O1 = 2.483(3) Å. The Eu–O bond

lengths with the hfac anions are in the range of 2.383(3)–2.458(3) Å. The Eu-O bond length with the water molecule is $\text{Eu1-O2} = 2.469(3)$ Å. The water molecule is involved in hydrogen interactions with oxygen atoms of hfac anions belonging to a neighboring molecule generating supramolecular dimers (Figure 3b). The distances for these interactions are: $(\text{O2})\text{-H1O}\cdots\text{O7}' = 2.177$ and $(\text{O2})\text{-H2O}\cdots\text{O4}' = 2.255$ Å. The corresponding angles are: $\text{O2-H1O}\cdots\text{O7}' = 146.8$ and $\text{O2-H2O}\cdots\text{O4}' = 151.8^\circ$ (symmetry code: $' = 1 - x, 1 - y, 1 - z$).

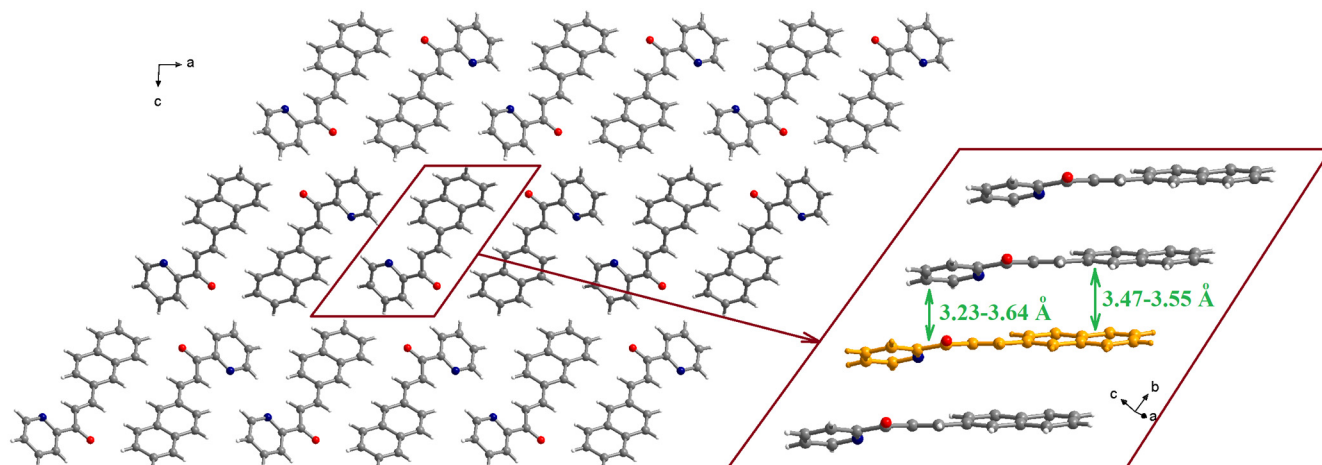


Figure 2. Packing diagram in the crystal structure of L (view along the crystallographic *b* axis). The inset shows details of the π - π stacking interactions within a pile running along the crystallographic *b* axis.

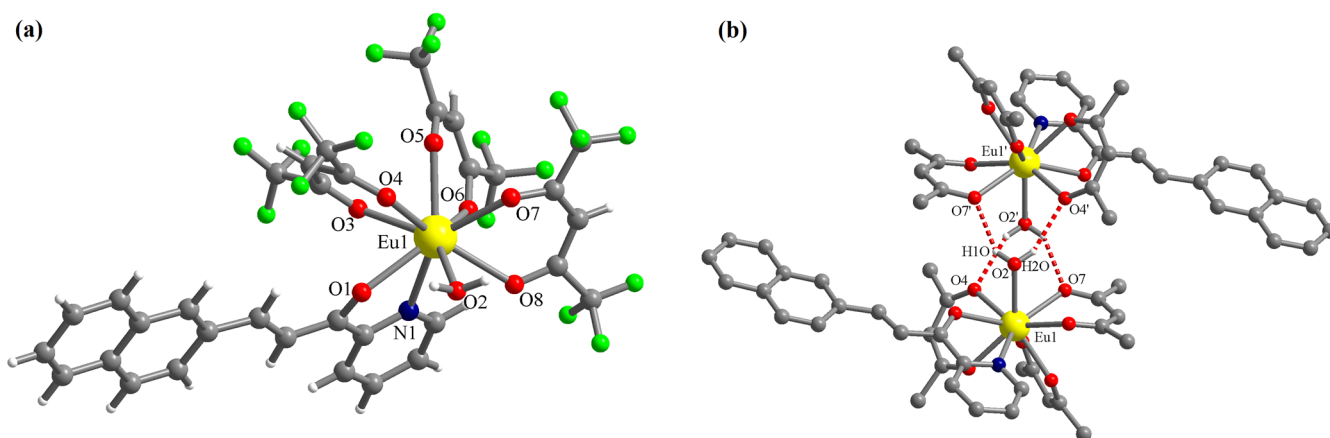


Figure 3. Perspective views of the molecular structure of the complex $[\text{Eu}(\text{L})(\text{hfac})_3(\text{H}_2\text{O})]$ (a) and of the supramolecular dimers generated by hydrogen interactions involving the coordinated water molecule (b)—the H and F atoms of the organic ligands were omitted for clarity; symmetry code: $' = 1 - x, 1 - y, 1 - z$).

The chalcone ligands from adjacent complexes are involved in π - π interactions (Figure 4). Two different patterns of overlapping can be observed. The first comprises only the naphthalene fragments, 3.55–3.59 Å, and the second consists in interactions between the pyridine and the naphthalene fragments, 3.45–3.58 Å (the insets from Figure 4).

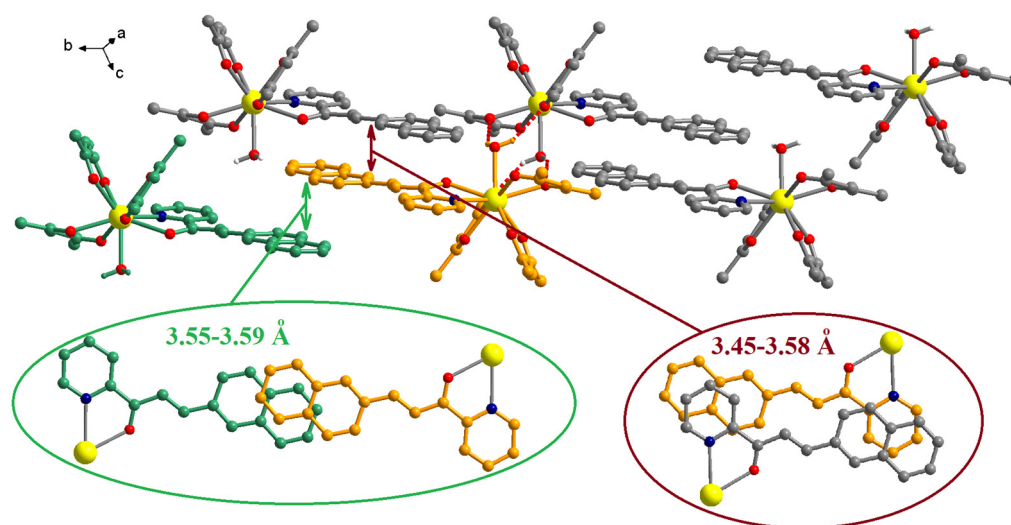


Figure 4. Packing diagram in crystal C1. The insets show details of the π - π interactions established by the chalcone ligands. The H and F atoms of the organic ligands were omitted for clarity.

The Tb(III) complex (C2) is not isostructural with the Eu(III) one. It also crystallizes in the triclinic $P-1$ space group, but the asymmetric unit contains two complexes with the formula $[\text{Tb}(\text{L})(\text{hfac})_3]$ and no solvent molecules (Figure 5). The Tb(III) ions are octacoordinated with three hfac anions and one chalcone L (the four ligands coordinate chelating bidentate). The chalcone ligands coordinate through the pyridine N atom and the ketone O atom. The corresponding bond lengths are: Tb1-N1 = 2.546(4), Tb2-N2 = 2.557(5), Tb1-O1 = 2.427(3), and Tb2-O8 = 2.425(4) Å. The Tb-O bond lengths with the hfac anions are in the range of 2.318(4)–2.396(4) Å.

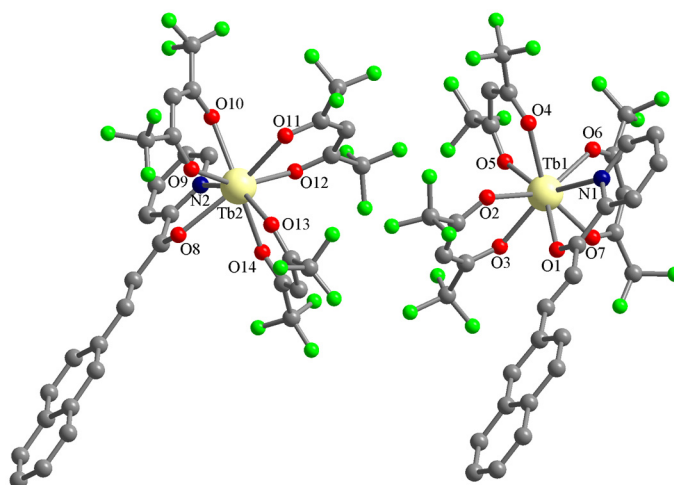


Figure 5. Perspective views of the asymmetric unit in crystal C2. The hydrogen atoms of the organic ligands were omitted for clarity.

The examination of the packing diagrams shows an organization in layers of the complexes in the crystallographic ab plane (Figure 6). Within the layers, a segregation of the two types of ligands can be observed. The chalcone ligands form piles along the crystallographic b axis by π - π interactions. There are three different types of π - π interactions with separation of 3.40–3.63, 3.44–3.65, and 3.50–3.62 Å. Details of the overlapping modes are presented in the insets of Figure 6. The CF_3 groups of hfac ligands establish $\text{F}\cdots\text{F}$ interactions generating fluorinated pillars that also run along the crystallographic b axis (Figure 6). The most $\text{F}\cdots\text{F}$ interactions are in the 2.82–3.24 Å range (Table 2). These values correspond with the $\text{F}\cdots\text{F}$ interactions reported as a driving force for the self-assembly of fluorinated compounds [23]

and, also, are similar to values found by us in other lanthanide(III) complexes with hfac ligands [24].

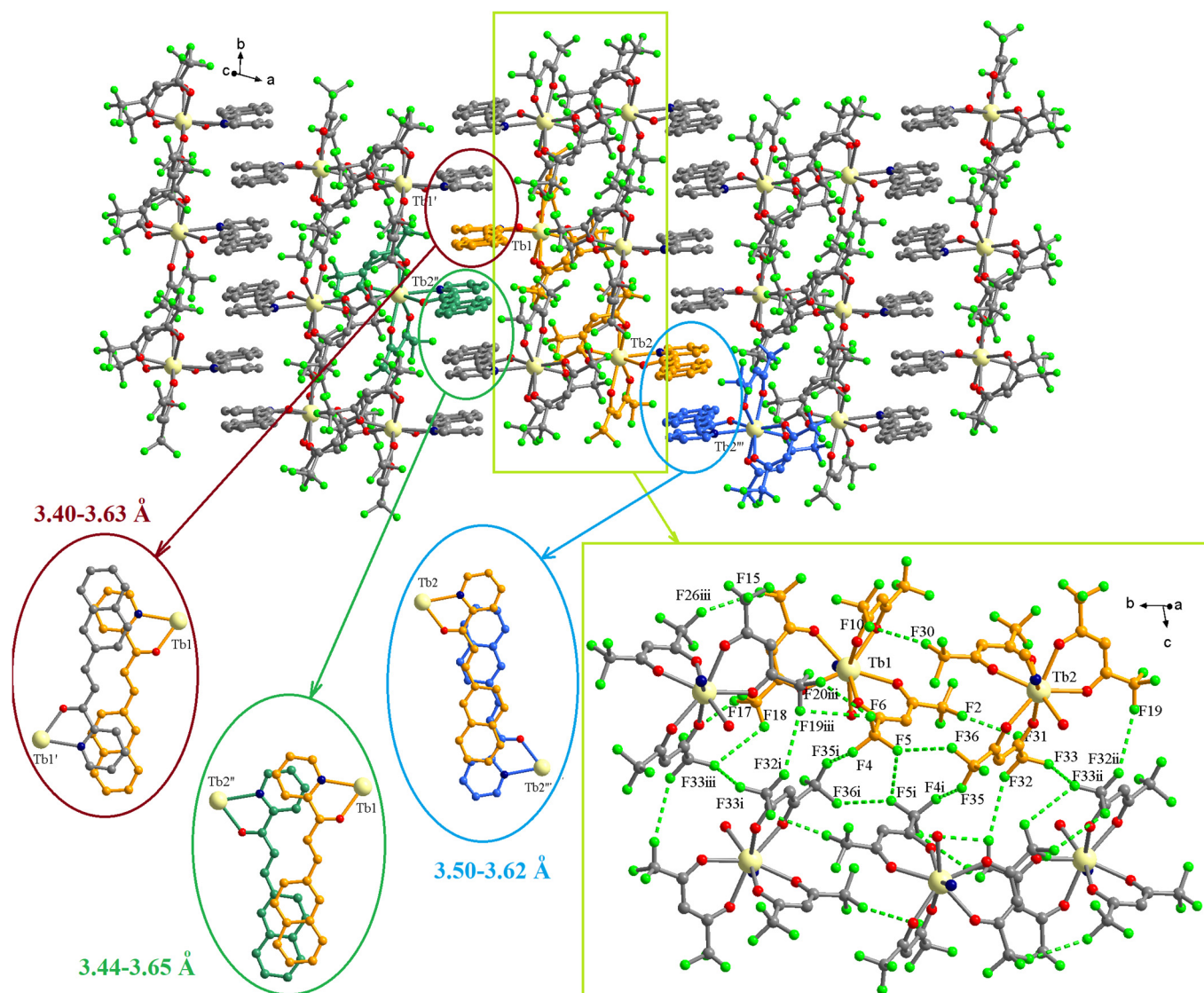


Figure 6. Packing diagram in crystallographic *ab* plane for the complex C2. The insets show details of the π - π and F...F interactions. Symmetry codes: $' = -x, 1 - y, 1 - z$; $'' = -1 + x, y, z$; $''' = 2 - x, -y, 1 - z$; $^i = 1 - x, 1 - y, 1 - z$; $^{ii} = 1 - x, -y, 1 - z$; $^{iii} = x, 1 + y, z$.

Table 2. Distances for the F...F interactions in the crystal C2 (Å).

| | | |
|-------------------------------|---------------------------------|--|
| F2...F31 = 2.821 | F6...F19 ⁱⁱⁱ = 3.238 | F15...F26 ⁱⁱⁱ = 3.051 |
| F5...F36 = 3.015 | F6...F20 ⁱⁱⁱ = 3.007 | F17...F26 ⁱⁱⁱ = 3.237 |
| F5...F5 ⁱ = 3.167 | F10...F30 = 3.046 | F18...F33 ⁱⁱⁱ = 3.153 |
| F4...F35 ⁱ = 2.894 | F19...F32 ⁱⁱ = 3.059 | F33 ⁱ ...F33 ⁱⁱⁱ = 2.900 |

Symmetry codes: $^i = 1 - x, 1 - y, 1 - z$; $^{ii} = 1 - x, -y, 1 - z$; $^{iii} = x, 1 + y, z$.

3.2. Spectral Properties

The optical properties of the ligand and complexes were studied only in a solid state because a partial dissociation of the complexes was observed in solution.

The absorption spectra of the ligand (L) and complexes (C1 and C2) were acquired on powder (using the diffuse reflectance technique) in the 200–1000 nm wavelength range. The absorption spectrum of the ligand presents an asymmetric band with maximum absorption at 416 nm and three shoulders at 314, 266, and 217 nm (Figure S2). The complexes

show broad absorption bands with maxima at 435 nm (C1) and 445 nm (C2) (Figure S3). Both complexes also present smaller absorption bands with maxima at 613 nm (C1) and 602 nm (C2). These bands are relatively broad, suggesting that they are not generated by f-f transitions.

The room temperature photoluminescence of ligand and complexes was investigated on powder and, for excitation, different wavelengths in the 300–400 nm range were used. The ligand has two emission bands partially overlapped with maxima at 490 and 522 nm (Figure 7a). The photoluminescence of the $[\text{Eu}(\text{L})(\text{hfac})_3(\text{H}_2\text{O})]\cdot 0.5\text{CHCl}_3$ and $[\text{Tb}(\text{L})(\text{hfac})_3]$ complexes depends on the radiation wavelength used for excitation (Figure 7b,c). In the 320–350 nm range, a strong sensitization of lanthanide emission via the ligand was observed. For the $[\text{Eu}(\text{L})(\text{hfac})_3(\text{H}_2\text{O})]\cdot 0.5\text{CHCl}_3$ complex, the strongest emission band was observed at 613 nm (${}^5\text{D}_0 - {}^7\text{F}_2$), and weaker bands appear at 592 nm (${}^5\text{D}_0 - {}^7\text{F}_1$) and 580 nm (${}^5\text{D}_0 - {}^7\text{F}_0$) [25]. The $[\text{Tb}(\text{L})(\text{hfac})_3]$ complex has the strongest emission at 546 nm (${}^5\text{D}_4 - {}^7\text{F}_5$) and weaker bands at 491 nm (${}^5\text{D}_4 - {}^7\text{F}_6$), and 584 nm (${}^5\text{D}_4 - {}^7\text{F}_4$). The efficiency of the antenna effect decreases for excitation wavelengths higher than 360–370 nm [26]. In the case of the Eu(III) complex (C1), the photoluminescence of the ligand is observed as a broad band with maximum around 510 nm for excitation wavelengths of 380–400 nm.

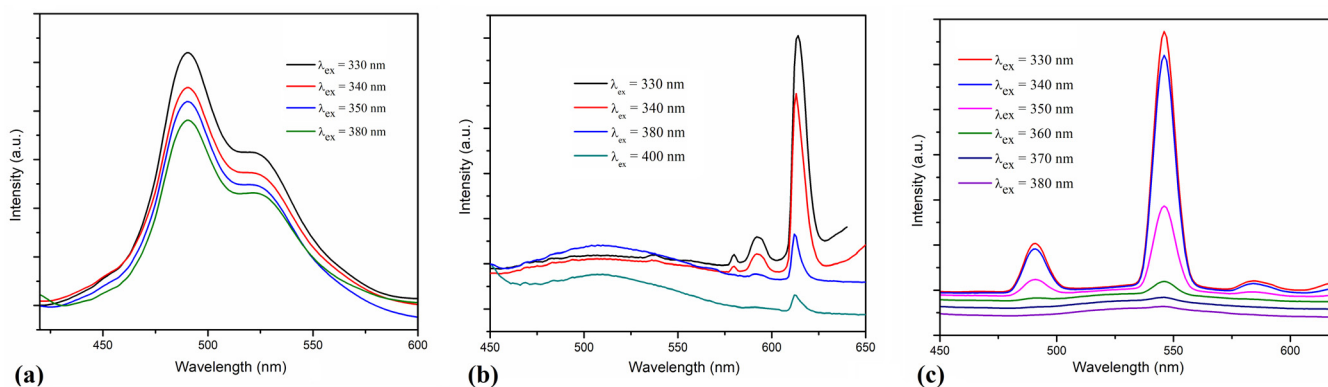


Figure 7. The emission spectra of the ligand L (a), and of the complexes $[\text{Eu}(\text{L})(\text{hfac})_3(\text{H}_2\text{O})]\cdot 0.5\text{CHCl}_3$ (b) and $[\text{Tb}(\text{L})(\text{hfac})_3]$ (c) obtained by excitation at various wavelengths on solid samples.

4. Conclusions

The chalcone ligand derived from 2-acetylpyridine and 2-naphthaldehyde is able to coordinate chelating bidentate to lanthanide ions in the presence of electron-withdrawing coligands (hexafluoroacetylacetonate anions). For these heteroleptic mononuclear complexes, the emission of the Eu(III) and Tb(III) ions was influenced by the excitation wavelength. As a further development of this project, we intend to expand the series of complexes with other lanthanide ions and other chalcone ligands. Exploration of the magnetic properties of the complexes is also envisaged.

Supplementary Materials: The following supporting information can be downloaded at: <https://www.mdpi.com/article/10.3390/cryst13091406/s1>, Figure S1: The ${}^1\text{H-NMR}$ spectrum of chalcone L ($\text{DMSO-}d_6$); Figure S2: The solid-state absorption spectrum of the ligand L; Figure S3: The solid-state absorption spectra of the complexes $[\text{Eu}(\text{L})(\text{hfac})_3(\text{H}_2\text{O})]\cdot 0.5\text{CHCl}_3$ (C1) and $[\text{Tb}(\text{L})(\text{hfac})_3]$ (C2); Figure S4: Comparison between the experimental (in blue) and single-crystal simulated (in red) XRPD patterns of the chalcone L; Figure S5: Comparison between the experimental (in red) and single-crystal simulated (in blue) XRPD patterns of the complex $[\text{Eu}(\text{L})(\text{hfac})_3(\text{H}_2\text{O})]\cdot 0.5\text{CHCl}_3$; Figure S6: Comparison between the experimental (in blue) and single-crystal simulated (in red) XRPD patterns of the complex $[\text{Tb}(\text{L})(\text{hfac})_3]$.

Author Contributions: Conceptualization, A.M.M.; methodology, V.L.V., A.H. and A.M.M.; synthesis, V.L.V.; formal analysis, V.L.V., A.H. and A.M.M.; investigation, V.L.V., A.H. and A.M.M.; writing—original draft preparation, A.M.M.; writing—review and editing, A.M.M. All authors have read and agreed to the published version of the manuscript.

Funding: This research received no external funding.

Data Availability Statement: Not applicable.

Conflicts of Interest: The authors declare no conflict of interest.

References

1. Zhuang, C.; Zhang, W.; Sheng, C.; Zhang, W.; Xing, C.; Miao, Z. Chalcone: A Privileged Structure in Medicinal Chemistry. *Chem. Rev.* **2017**, *117*, 7762–7810. [[CrossRef](#)]
2. Huang, H.; Wu, W.; Zhu, K.; Hu, J.; Ye, J. Highly Diastereo- and Enantioselective Cross-Cascade Reactions of Different Enones. *Chem. Eur. J.* **2013**, *19*, 3838–3841. [[CrossRef](#)] [[PubMed](#)]
3. Wu, J.; Leng, W.L.; Liao, H.; Hoang, K.L.M.; Liu, X.-W. Intramolecular C-N Bond Formation under Metal-free Conditions: Synthesis of Indolizines. *Chem. Asian J.* **2015**, *10*, 853–856. [[CrossRef](#)] [[PubMed](#)]
4. Reddy, P.L.; Kumar, K.P.; Satyanarayana, S.; Narender, R.; Reddy, B.V.S. An efficient synthesis of 2-aryl-1,4-diketones via hydroacylation of enones. *Tetrahedron Lett.* **2012**, *53*, 1546–1549. [[CrossRef](#)]
5. Cordaro, J.G.; McCusker, J.K.; Bergman, R.G. Synthesis of mono-substituted 2,2'-bipyridines. *Chem. Commun.* **2002**, *14*, 1496–1497. [[CrossRef](#)]
6. Zhao, Y.; Li, H.; Shao, Z.; Xu, W.; Meng, X.; Song, Y.; Hou, H. Investigation of Regulating Third-Order Nonlinear Optical Property by Coordination Interaction. *Inorg. Chem.* **2019**, *58*, 4792–4801. [[CrossRef](#)]
7. Ray, D.; Nag, A.; Goswami, D.; Bharadwaj, P.K. Acyclic donor-acceptor-donor chromophores for large enhancement of two-photon absorption cross-section in the presence of Mg(II), Ca(II) or Zn(II) ions. *J. Lumin.* **2009**, *129*, 256–262. [[CrossRef](#)]
8. Diwan, U.; Kumar, A.; Kumar, V.; Upadhyay, K.K. Solvent viscosity tuned highly selective NIR and ratiometric fluorescent sensing of Fe³⁺ by a symmetric chalcone analogue. *Dalton Trans.* **2013**, *42*, 13889–13896. [[CrossRef](#)]
9. Cheng, X.; Zhang, H.; Ye, K.; Zhang, H.; Wang, Y. Morphology-dependent fluorescence ON/OFF of a beryllium complex: ACQ in amorphous solids, AEE in crystalline powders and the dark/bright fluorescence switch. *J. Mater. Chem. C* **2013**, *1*, 7507–7512. [[CrossRef](#)]
10. Gaur, R.; Mishra, L. Supramolecular and theoretical investigation of copper(II) complexes containing 2,2'-bipyridine and substituted chalcone ligands: Estimation of non-covalent interactions. *J. Mol. Struct.* **2023**, *1273*, 134271. [[CrossRef](#)]
11. Křikavová, R.; Vančo, J.; Trávníček, Z.; Hutýra, J.; Dvořák, Z. Design and characterization of highly in vitro antitumor active ternary copper(II) complexes containing 2'-hydroxychalcone ligands. *J. Inorg. Biochem.* **2016**, *163*, 8–17. [[CrossRef](#)] [[PubMed](#)]
12. Kahrović, E.; Zahirović, A.; Višnjevac, A.; Osmanković, I.; Turkušić, E.; Kurtagić, H. Chalcone and Flavonol Copper(II) Complexes Containing Schiff Base Co-Ligand: Synthesis, Crystal Structures and Catecholase-like Activity. *Croat. Chem. Acta* **2018**, *91*, 195–207. [[CrossRef](#)]
13. Gaur, R.; Choubey, D.K.; Usman, M.; Ward, B.D.; Roy, J.K.; Mishra, L. Synthesis, structures, nuclease activity, cytotoxicity, DFT and molecular docking studies of two nitrate bridged homodinuclear (Cu-Cu, Zn-Zn) complexes containing 2,2'-bipyridine and a chalcone derivative. *J. Photochem. Photobiol. B Biol.* **2017**, *173*, 650–660. [[CrossRef](#)]
14. Li, X.; Sun, H.; Flörke, U.; Klein, H.-F. α,β -Unsaturated Carbonyl Compounds as Hard/Soft Chelating Ligands in Methyl Nickel Phenolates and the Structure of trans-Methyl-2-(3-phenyl-2,3- η^2 -propenoyl)phenolatobis(trimethylphosphine)nickel(II). *Organometallics* **2005**, *24*, 4347–4350. [[CrossRef](#)]
15. Zahirović, A.; Roca, S.; Višnjevac, A.; Kahrović, E. Ruthenium organometallics of chloro-substituted 2'-hydroxychalcones—A story of catecholase biomimetics beyond copper. *J. Organomet. Chem.* **2021**, *945*, 121863. [[CrossRef](#)]
16. Zahirović, A.; Roca, S.; Kahrović, E.; Višnjevac, A. Low DNA and high BSA binding affinity of cationic ruthenium(II) organometallic featuring pyridine and 2'-hydroxychalcone ligands. *J. Mol. Struct.* **2021**, *1236*, 130326. [[CrossRef](#)]
17. Prajapati, R.; Dubey, S.K.; Gaur, R.; Koiri, R.K.; Maurya, B.K.; Trigun, S.K.; Mishra, L. Structural characterization and cytotoxicity studies of ruthenium(II)-dmsO-chloro complexes of chalcone and flavone derivatives. *Polyhedron* **2010**, *29*, 1055–1061. [[CrossRef](#)]
18. Gaur, R.; Mishra, L. Synthesis and Characterization of Ru(II)-DMSO-Cl-Chalcone Complexes: DNA Binding, Nuclease, and Topoisomerase II Inhibitory Activity. *Inorg. Chem.* **2012**, *51*, 3059–3070. [[CrossRef](#)]
19. Balázs, L.B.; Tay, W.S.; Pullarkat, S.A.; Leung, P.-H. Synthesis of Stereoprojecting, Chiral N-C(sp³)-E Type Pincer Complexes. *Organometallics* **2018**, *37*, 2272–2285. [[CrossRef](#)]
20. Abbas, Z.; Dasari, S.; Patra, A.K. Ternary Eu(III) and Tb(III) β -diketonate complexes containing chalcones: Photophysical studies and biological outlook. *RSC Adv.* **2017**, *7*, 44272–44281. [[CrossRef](#)]
21. Marqués-Gallego, P.; den Dulk, H.; Brouwer, J.; Kooijman, H.; Spek, A.L.; Roubeau, O.; Teat, S.J.; Reedijk, J. Synthesis, Crystal Structure, Studies in Solution and Cytotoxicity of Two New Fluorescent Platinum(II) Compounds Containing Anthracene Derivatives as a Carrier Ligand. *Inorg. Chem.* **2008**, *47*, 11171–11179. [[CrossRef](#)] [[PubMed](#)]
22. Bernot, K.; Bogani, L.; Caneschi, A.; Gatteschi, D.; Sessoli, R. A Family of Rare-Earth-Based Single Chain Magnets: Playing with Anisotropy. *J. Am. Chem. Soc.* **2006**, *128*, 7947–7956. [[CrossRef](#)] [[PubMed](#)]
23. Janjić, G.V.; Jelić, S.T.; Trišović, N.P.; Popović, D.M.; Đorđević, I.S.; Milčić, M.K. New Theoretical Insight into Fluorination and Fluorine-Fluorine Interactions as a Driving Force in Crystal Structures. *Cryst. Growth Des.* **2020**, *20*, 2943–2951. [[CrossRef](#)]
24. Popa, A.D.; Răducă, M.; Mădălan, A.M. Luminescent La³⁺, Eu³⁺ and Tb³⁺ mononuclear complexes with a Schiff base tripodal ligand derived from 9-anthracenecarboxaldehyde. *Polyhedron* **2023**, *239*, 116441. [[CrossRef](#)]

25. Pasatoiu, T.D.; Madalan, A.M.; Kumke, M.U.; Tiseanu, C.; Andruh, M. Temperature Switch of LMCT Role: From Quenching to Sensitization of Europium Emission in a Zn^{II}-Eu^{III} Binuclear Complex. *Inorg. Chem.* **2010**, *49*, 2310–2315. [[CrossRef](#)]
26. Pasatoiu, T.D.; Tiseanu, C.; Madalan, A.M.; Jurca, B.; Duhayon, C.; Sutter, J.P.; Andruh, M. Study of the Luminescent and Magnetic Properties of a Series of Heterodinuclear [Zn^{II}Ln^{III}] Complexes. *Inorg. Chem.* **2011**, *50*, 5879–5889. [[CrossRef](#)]

Disclaimer/Publisher's Note: The statements, opinions and data contained in all publications are solely those of the individual author(s) and contributor(s) and not of MDPI and/or the editor(s). MDPI and/or the editor(s) disclaim responsibility for any injury to people or property resulting from any ideas, methods, instructions or products referred to in the content.